ELSEVIER

Bioelectrochemistry and Bioenergetics 46 (1998) 105–114

BIOELECTROCHEMISTRY AND BIOENERGETICS

# The influence of electrode polarisation on dielectric spectra, with special reference to capacitive biomass measurements: (II) Reduction in the contribution of electrode polarisation to dielectric spectra using a two-frequency method

Christopher L. Davey *, Douglas B. Kell

*Institute of Biological Sciences, University of Wales, Aberystwyth, Ceredigion, Wales, SY23 3DA, UK*

Received 30 May 1998; accepted 9 June 1998

**Abstract**

Electrode polarisation can interfere significantly with the measurement of the dielectric properties of biological systems, and in particular with the dielectric estimation of microbial biomass. We showed in the previous paper of this pair [C.L. Davey, D.B. Kell, The influence of electrode polarisation on dielectric spectra, with special reference to capacitive biomass measurements: I. Quantifying the effects on electrode polarisation of factors likely to occur during fermentations, Bioelectrochem. Bioenerg., 1998] that electrode polarisation can be modelled by a power law and that the parameters of this model can be simply modified to give reliable and intuitive measures of the magnitude ($^{L}C_{p}$) and rate of fall of polarisation with increasing frequency ($^{h}f$). Importantly and surprisingly, although the *magnitude* of electrode polarisation can change it was found that the $^{h}f$ value remained constant. A highly useful consequence of this constancy of $^{h}f$ for a given instrument is that one can exploit it directly to eliminate electrode polarisation from biological capacitance (or permittivity) spectra using the simple two-frequency method developed in this paper. 

*Keywords:* Dielectric spectroscopy; Electrode polarisation; Biomass estimation

## 1. Introduction

As was discussed in the previous paper in this pair [1] electrode polarisation can be a major limiting factor in the present applications of capacitive biomass measurements [2–4] and dielectric spectroscopy in general [5–9]. The problem can become particularly serious when working at frequencies below 100 kHz [10] and this has prevented detailed empirical studies of the dielectric properties of cells under anything like physiological conditions at these frequencies [11]. This in turn has prevented the use of these low-frequency properties in fermenter monitoring systems and in many medical applications. As most of the more interesting electric field effects that are thought to occur with biosystems are also at these low frequencies [12] there is also a lack of the detailed information required to refine the models of these processes.

There is thus a great need for a method of reducing the contribution of electrode polarisation to dielectric spectra. In this paper we develop such a method and exploit it to reduce the detrimental influence of electrode polarisation on capacitive biomass measurements with particular reference to measurements made with the Aber Instruments Biomass Monitor (BM). A variety of methods have been used in the past to remove the electrode polarisation's contribution to biological capacitance spectra with varying degrees of practicality for fermentation measurements. These methods are discussed below.

(1) Taking measurements with different distances between the measuring electrodes whilst keeping the electrode surface current density constant [7]. As the distance changes, the electrode polarisation's impedance remains the same whilst the suspension's impedance changes, enabling one to eliminate the polarisation's contribution to the signal. This method is impractical for on-line biomass measurements as it involves introducing potentially unreliable moving parts into the fermenter, although a vibrating electrode system may be possible.

* Corresponding author

0302-4598/98/$19.00 

(2) One can do a frequency scan of the β-dispersion with the electrode polarisation present. Non-linear least squares curve fitting is then used to fit the data to the Cole–Cole equation for the β-dispersion and a term modeling the polarisation [13,14]. This gives a best estimate value for the dielectric increment of the β-dispersion ($\Delta C_\beta$ [1]) which can be used for biomass estimation. For the Biomass Monitor (BM) the limited frequency range (0.2 to 10 MHz) combined with some residual uncompensated inductances at the higher frequencies means that this method ceases to be reliable at the large polarisations of interest in this paper.

(3) The polarisation control method [6,7,10] is frequently used for off-line measurements done on the BM. This involves doing a frequency scan of the cell suspension whilst noting down the conductance at the lowest frequency used. One then takes a sample of the suspending medium and adjusts its conductance, at the lowest frequency, to that of the suspension using distilled water or KCl. A scan of this solution gives one an estimate of the polarisation which can subsequently be subtracted from the cell suspension scan to give data largely free from polarisation. This method however cannot be put on-line in a fermenter.

(4) Inductively coupled electrodes can eliminate the need for actual physical contact between the metal used in the measuring system and the aqueous ionic suspension medium, thus removing polarisation completely. Although such systems do exist [4] none of them as yet have been developed enough to be a useful proposition in a real fermentation environment.

(5) Non-polarisable electrodes can be used and indeed the BM used solid pure gold electrode pins. As was shown in Ref. [1] the recent move to platinum pins for BM probes will result in significant reductions in electrode polarisation [7]. Even platinum, however, does not reduce polarisation enough to allow reliable measurements at very high conductances with a relatively low biomass concentration present.

(6) The BM's main method of reducing electrode polarisation is the use of a four-electrode pin system [5,7,15–18]. The two outer pins are used to drive current though the sample whilst the two inner pins are used to detect the potential drop across the suspension that this induces. This potential is detected with a very high impedance voltmeter system which means that virtually no current flows across the inner pins' electrode/solution interfaces. As it is such a current flow that causes the polarisation then its elimination also removes the polarisation problem. In practice, the four-terminal electrode configuration works well when compared to say a pair of platinum blacked platinum pins [11,18,19] but it does not remove all the polarisation, especially in highly conducting media.

The BM's phase detector system is capable of accurately detecting very small capacitance values in the presence of a large conductance [15]. What limits its use at the high conductances found in animal cell suspensions and in some microbial broths is the electrode polarisation present. For suspensions with a high biomass content, as in some immobilised systems or high-density cultures, electrode polarisation is not a significant problem even at high conductances. Where a new polarisation elimination method would be useful is in those situations where the β-dispersion curve has become embedded in a large polarisation curve because the biomass concentration is relatively low. The aim of the work described in this paper was to address this problem by building on the findings of the previous paper in this pair [1].

## 2. Methods

Unless otherwise stated the methods and equipment were exactly as those used in Ref. [1].

### 2.1. Yeast used

The living yeast suspensions used were made using fresh baker's yeast paste obtained locally. When the BM was in high cell constant mode the yeast was made up in 140 mM KCl, in low cell constant mode 70 mM was used. The suspensions were made as follows. (1) The extent of electrode polarisation in the relevant KCl solution was estimated by measuring the difference in capacitance between 0.2 and 1 MHz. (2) The BM was then set to 0.4 MHz and yeast paste added and suspended until the capacitance had increased by between one half and one times the estimated polarisation magnitude. (3) The suspension was then left an hour to stabilise. This resulted in a suspension where the yeast β-dispersion was well-embedded in the electrode polarisation but was still visible under it.

### 2.2. Electrical measurements

The experiments on live yeast (and their polarisation controls) used the gold-pinned probe with the matt surfaces (mAu probe) used in [1]. Thirty-three frequencies were picked to place the majority of the data points in the frequency region where the polarisation and yeast β-dispersion overlapped most. The scans were done under manual control and the results were written down from the BM display. The order of the frequencies was differently randomised for each scan. The BM set-up was the same as in Ref. [1] apart from the fact that the 5-second time constant low-pass filter was used where noise fluctuations were a problem and that scans were done in high and low cell constant modes. Polarisation controls were done by adjusting the 0.2 MHz conductance of distilled water using solid KCl so that it had the same 0.2 MHz conductance as the relevant yeast suspension (see Section 1 for details).

## 3. Results and discussion

### *3.1. Using the constant $^{h}f$ value to reduce electrode polarisation by the use of a 2 frequency (2f) method*

In [1] it was shown that electrode polarisation can be modeled by a power law and that the parameters of this model can be simply modified to give reliable and intuitive measures of magnitude ($^{L}C_{p}$) and rate of fall of *polarisation* with increasing frequency ($^{h}f$). It was further shown that above a certain value of conductance (3–7 mS) the $^{h}f$ was constant.

A most useful consequence of this constant $^{h}f$ (the value of which may vary from BM to BM or more likely between different electrode geometries/constructions) is that one can exploit it to eliminate electrode polarisation from biological capacitance (or permittivity) spectra rather directly, without the need, for example to use artificial neural network or chemometric models [20,21]. The principle of this method is illustrated on Fig. 1. What is shown is the β-dispersion (on its instrumental baseline) that one is trying to measure (line a), along with the same dispersion embedded in electrode polarisation as one might measure in reality (line b). What one would like to do is take some spot capacitance readings and use these to estimate the way the polarisation falls with frequency. Having done this one would subtract this calculated polarisation curve from the measured capacitance spectrum (line b) to leave the underlying β-dispersion (plus baseline) uncontaminated by polarisation (line a). For most of the β-dispersions one would wish to study or use to quantify the biomass concentration, the values of $f_c$ are such that one is largely on the low-frequency plateau by the time the frequency falls below about 0.3 MHz (see later for a detailed discussion of this). Under these conditions one can take a spot capacitance measurement at $^{L}f$ (typically $2.10^{5}$ Hz). This measured capacitance is called $^{L}C_{m}$ and from Fig. 1 it is given by:

$$^{L}C_{m} = {}^{c}C_{o} + {}^{L}C_{p} \quad (1)$$

where $^{c}C_{o}$ is the capacitance offset under the polarisation curve (in pF) which is made-up of the β-dispersion plateau and any equipment baseline offsets. If one takes another spot capacitance measurement at the half frequency to give $^{h}C_{m}$ (in pF) we see from Fig. 1 that this is given by:

$$^{h}C_{m} = {}^{c}C_{o} + \frac{^{L}C_{p}}{2} \quad (2)$$

where $^{c}C_{o}$ is the same as before. This pair of simultaneous equations is easily solved by subtracting Eq. (2) from Eq. (1) to give Eq. (3).

$$^{L}C_{p} = 2\left(^{L}C_{m} - {}^{h}C_{m}\right) \quad (3)$$

For this method the offset is taken as *any* capacitance that the polarisation curve sits on and is usually made up of the β-dispersion curve and the instrument's (BM) baseline. Note that for all this paper a constant offset refers to the fact that the offset is identical at $^{L}f$ and $^{h}f$, at other frequencies (including those between $^{L}f$ and $^{h}f$) the offset may well change.

As one selects $^{L}f$ oneself and $^{h}f$ is a known constant (relative to it) one can take spot measurements of the capacitance of the suspension at these frequencies (to give $^{L}C_{m}$ and $^{h}C_{m}$, respectively). Eq. (3) then gives the magnitude of the electrode polarisation at $^{L}f$, i.e., $^{L}C_{p}$ (see Fig. 8 in [1]). To calculate how this polarisation capacitance falls as frequency increases one needs to use the measures of the rate of fall of capacitance with increasing frequency, namely $p$ or $^{h}f$ [1]. As we have consistently been using $^{h}f$, and as its use only slightly increases the complexity of the algebra, the equation describing the fall in polarisation capacitance in the BM's frequency range was derived for this. Appendix A gives the derivation of Eq. (4) which describes the fall in polarisation capacitance ($^{f}C_{p}$) in terms of the applied frequency $f$, $^{L}f$, $^{h}f$ (all in Hz) and $^{L}C_{p}$ (in pF).

$$^{f}C_{p} = {}^{L}C_{p}\,2^{\left(\log\left(^{L}f/f\right)/\log\left(^{h}f/^{L}f\right)\right)} \quad (4)$$

Thus having obtained $^{L}C_{p}$ from Eq. (3), one can vary $f$ in Eq. (4) to generate the electrode polarisation curve. This curve can then be subtracted from the full biological

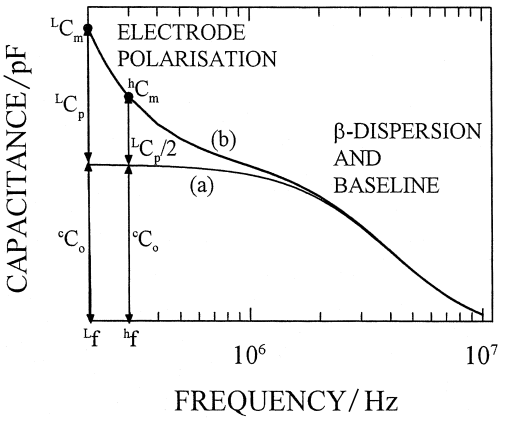


Fig. 1. The principle behind the 2f method of reducing electrode polarisation. (a) A β-dispersion curve superpositioned on the spectrometers baseline and reaching its low-frequency plateau at the frequencies used to estimate the electrode polarisation. (b) The curve in (a) with electrode polarisation present and represents the capacitance a spectrometer would measure ($^{f}C_{m}$) as it changes the frequency. At the lowest frequency used for the scan ($^{L}f$) the capacitance measured ($^{L}C_{m}$) is made up of the 'constant' offset capacitance $^{c}C_{o}$ (due to the β-dispersion and BM baseline) and our measure of the magnitude of the polarisation $^{L}C_{p}$. At the known half frequency ($^{h}f$) the capacitance measured is $^{h}C_{m}$. The magnitude of the polarisation capacitance has by definition halved to $^{L}C_{p}/2$ and the offset capacitance is still $^{c}C_{o}$. By taking spot measurements of capacitance at $^{L}f$ and $^{h}f$ to give $^{L}C_{m}$ and $^{h}C_{m}$, respectively, one can calculate the polarisation curve using the equations in the text. This polarisation curve can then be subtracted from line (b) to give the polarisation free line (a).

spectrum (line b in Fig. 1) to give the polarisation-free β-dispersion on its BM baseline (line a in Fig. 1).

### *3.2. Simulations of the effect of a sloping offset under the polarisation, on the 2f method*

The major limiting assumption underlying the 2f method is that it assumes the capacitance offset ($^{c}C_{o}$) under the polarisation curve is the same at $^{L}f$ and $^{h}f$ (see Fig. 1). This may not be true within the BM's frequency range and especially if $^{L}f$ and $^{h}f$ values of 0.20 and 0.28 MHz, respectively, are used. A β-dispersion with a low $f_c$ and a significant Cole–Cole $\alpha$ value (e.g., animal cells [11,19,22]) may not fully reach the low-frequency plateau in the BM's frequency range (see Fig. 1 in Ref. [1]). Fig. 3a in Ref. [1] showed that the BM's baseline itself may slope in the frequency range of interest. Changes in the offset capacitance may also be caused by a noise spike effecting the capacitance data at one of the frequencies, or by the tail-end of a lower frequency dispersion such as an $\alpha$-dispersion.

Spreadsheet simulations of the effect of a sloping offset on the 2f method showed that the effects seen in Fig. 2 could be expected. Line (a) is a capacitance scan of a cell suspension contaminated by electrode polarisation. Line (b) is the offset under this polarisation and comprises the β-dispersion and any instrumental baseline effects. As one can see this offset drops significantly between the $^{L}f$ and $^{h}f$ shown on the plot. If spot measurements of the suspension capacitance were taken at $^{L}f$ and $^{h}f$ and the 2f model used to back-calculate the frequency dependence of the polarisation one does not get the true polarisation curve (line d). In fact one gets an over-estimation of the polarisation (line e) which when subtracted from the suspension spectrum (line a) does not give the true offset (line b) but a slightly distorted version (line c). This slight distortion does not cause a significant problem for biomass estimation if one uses a biomass measuring frequency (upward pointing arrow) slightly above the $^{h}f$ used, as illustrated on the figure. The downward pointing arrow highlights the significant reduction in the polarisation at the measuring frequency that the application of the 2f method has effected.

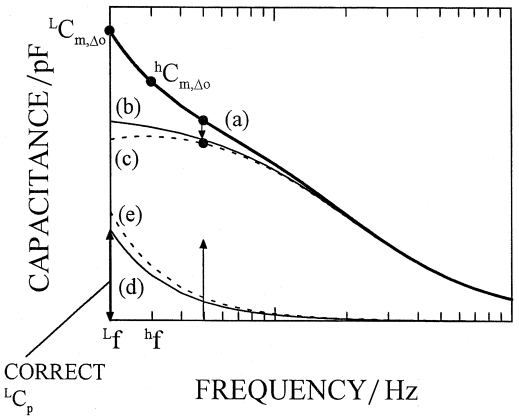


Fig. 2. The effect of a sloping offset at $^{L}f$ and $^{h}f$ on the 2f method of compensating for electrode polarisation. (a) The capacitance measured by the spectrometer when the offset slopes. The additional '$\Delta$o' terms in the subscripts indicate the offset changes between $^{L}f$ and $^{h}f$. The vertical arrow indicates a spot biomass measuring frequency. See the text for full details.

To investigate the effect that a non-constant offset might have on biomass measurements under realistic but controlled conditions, simulations were performed. For the simulations the $^{L}f$ used was $2.10^{5}$ Hz. As the simulations would be based on the results gained for the mAu probe the $^{h}f$ used would be taken from its data. The mAu $^{h}f$ values for all the scans where the conductance was $\geq 7$ mS in Ref. [1] were used. The mean (to the number of decimal places the BM offers) was 0.28 MHz (S.D. = 0.0061 MHz) and this was used as the $^{h}f$ for all the simulations. The use of an averaged $^{h}f$ would show-up any effects on the 2f method caused by real but slight differences in $^{h}f$. The chosen biomass measuring frequency was 0.4 MHz as this is typical of real biomass measurements. A set of simulations was generated using the data from the KCl concentration experiment in Ref. [1], by carrying out the following at *each* concentration.

(1) A set of simulated cell suspension data with a sloping offset was generated. For each KCl concentration two such sets were generated, each using β-dispersions with different $f_c$ values, as follows.

(a) To obtain a realistic BM baseline under the polarisation curve the actual straight line fitted to the probe dispersion at that concentration was used. Thus for the simulation equivalent to the 56 mM KCl data the straight line on Fig. 3a in Ref. [1] was used. In a real biomass measurement the capacitance of the uninoculated medium would be zeroed prior to the experiment. To simulate this the straight line was offset so that it crossed the abscissa at 0.4 MHz.

(b) Next β-dispersion data were simulated and added to the baseline generated in (a) to give the offset curve under the polarisation. At each KCl concentration the same pair of simulated β-dispersions were used to produce the pair of simulated data sets needed. The dispersions were generated using the Cole–Cole equation [10] using $\Delta C_{\beta} = 20$ pF, Cole–Cole $\alpha = 0.15$ and $C_{\infty} = 0$ and two different $f_c$ values. The lower $f_c$ value was 0.75 MHz and gave a realistic dispersion for large cells like animal cells. This low $f_c$ in combination with the large (but realistic) $\alpha$ value caused the dispersion to be significantly off the low-frequency plateau region over the frequency range of the BM simulated here (see Fig. 1 in Ref. [1]). The second dispersion had a higher $f_c$ of 1.5 MHz, which is typical of yeast cells.

(c) The polarisation curve used was the power law fitted to the real data at the KCl concentration of interest (from Ref. [1]). Thus for the 56 mM KCl simulation the $^{1Hz}C_{p}$ and $p$ values from the fitted line on Fig. 4 in Ref. [1] were

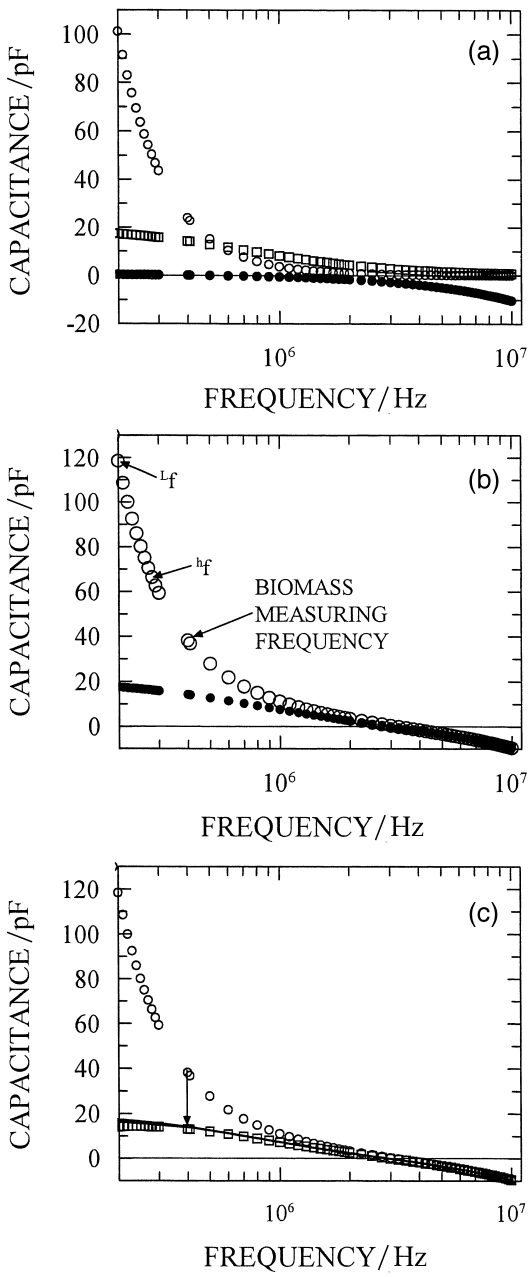


Fig. 3. Simulations of the effect a sloping offset has on the 2f method for the mAu probe and 175 mM KCl using the 0.75 MHz $f_c$ β-dispersion. (a) The components used to generate the simulation. Open circles is the polarisation used, closed circles the BM baseline and the squares the β-dispersion. (b) The data in (a) after being converted to a form suitable for testing the 2f method. The closed circles are the offset data created by adding the baseline and β-dispersion data in (a). It is this line that the 2f method should give if it works perfectly. The open circles are the simulation of the capacitances that a spectrometer would measure for a cell suspension and is formed by the addition of all the data in (a). This constitutes the test suspension data. The capacitances at $^{L}f$ and $^{h}f$ are then fed to the 2f method to allow compensation of the polarisation. (c) The results of applying the 2f method to the cell suspension data in (b). The open circles are the cell suspension data from (b) and the line is the offset data from (b). The squares are the results of applying the 2f method to the cell suspension as described in the text. The vertical arrow indicates the reduction in the polarisation's contribution to capacitance measured using a spot frequency of 0.4 MHz.

put into Equation 1 of Ref. [1] to generate the polarisation curve. This polarisation curve was then added to the two sets of offset data generated in (b) to give the required pair of simulated cell suspension data.

Fig. 3a shows the BM baseline data, β-dispersion ( $f_c$ = 0.75 MHz) and polarisation data equivalent to 175 mM KCl generated as above. Fig. 3b shows the resulting offset data and simulated suspension data resulting from the plots in a. Note how embedded the offset data (including the β-dispersion) are in the polarisation.

(2) Once the test suspension data had been generated (one set for each $f_c$ at each KCl concentration) each was then used to test the 2f method. The capacitance values at the fixed $^{L}f$ and $^{h}f$ were taken and inserted into Eq. (3) to give the 2f method's estimate of $^{L}C_p$. This value was then inserted into Eq. (4) to generate an estimate of the frequency dependence of the polarisation ($^{f}C_p$) which was then subtracted from the cell suspension data to give an estimate of the underlying offset curve free from polarisation. Fig. 3c shows the simulated cell suspension data from b along with the correct offset and the 2f method's estimate of this offset generated as above. It is seen that the estimated offset dips slightly below the real value at low frequencies but by the measuring frequency of 0.4 MHz it is very close to the true value. The arrow indicates just how much polarisation had been removed by the application of the 2f method to biomass estimation at 0.4 MHz. One should note that at 0.4 MHz the offset component due to the baseline of the BM is zero and so the offset capacitance is due entirely to the β-dispersion.

Fig. 4a and b summarise the results of the simulations for the two β-dispersion $f_c$ values used. On each plot are shown the simulated cell suspension capacitance values at the measuring frequency of 0.4 MHz, along with the correct offset (in this case β-dispersion) value at that frequency (line). The application of the 2f method to the simulated suspension data resulted in the estimates of the 0.4 MHz offset capacitances which are dotted along the correct value line. The 2f model thus seems to work for all the conductances above 7 mS. At the high conductances it accurately reveals the β-dispersion even though it is completely embedded in the polarisation data. At the other conductance extreme it effectively removes the polarisation even though the slope in the offset is significant compared to the magnitude of the polarisation present.

The reason the 2f method could not be applied to conductances below a few mS was that below this threshold the $^{h}f$ became conductance dependent due to instrumental artifacts (see Fig. 10 in Ref. [1]). It is entirely possible that these low conductance $^{h}f$ values are stable and so a calibration curve such as that in Fig. 10 in Ref. [1] could be used to read off the $^{h}f$ values to use in the 2f method at these low conductance values.

Follow-up simulations were done to investigate the effects of noise spikes disturbing one or other of $^{L}f$ and $^{h}f$ during frequency scanning. These were done exactly as

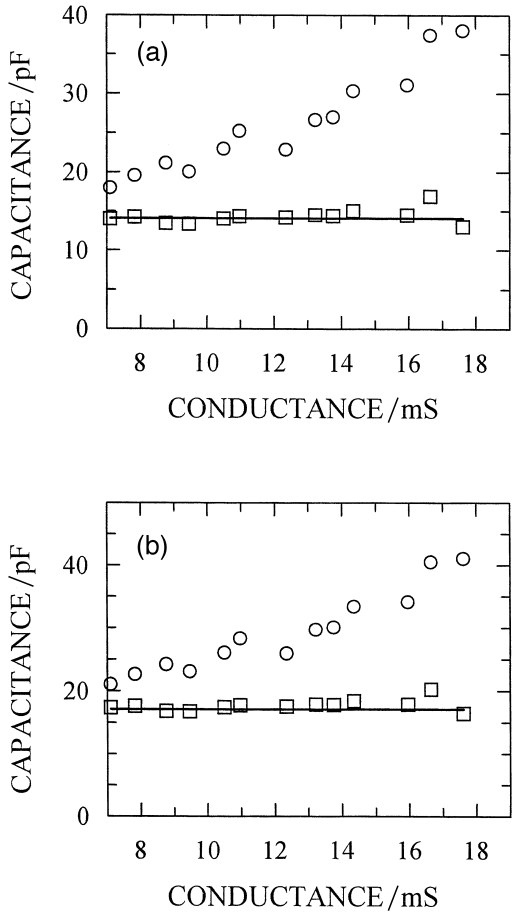


Fig. 4. Summaries of repeating the simulation in Fig. 3 over a wide range of conductances using the low frequency β-dispersion $f_c$ (a) and high frequency $f_c$ (b). On each plot the correct offset capacitance at the spot biomass measuring frequency (0.4 MHz) is shown by a line. At this frequency the baseline was offset to zero simulating the procedure used for real biomass measurements and so at this frequency the offset capacitance is due solely to the β-dispersion. The open circles are the capacitances at 0.4 MHz for the simulated cell suspension as indicated by the blunt end of the arrow on Fig. 3c. The squares are the estimates of the capacitance at 0.4 MHz resulting from the application of the 2f method as indicated by the square at the tip of the arrow on Fig. 3c.

above but only on the 120 mM KCl data (as this is in the mid-conductance range) and with the higher $f_c$ β-dispersion. After the simulated cell suspension data were generated the capacitances at ${}^{L}f$ or ${}^{h}f$ were altered before being fed into the 2f method. The estimated offset capacitances after using the 2f method to remove the polarisation were then compared to the real values as before. The following alterations were each given their own simulation, ${}^{L}C_m + 0.5\,pF$; ${}^{L}C_m - 0.5\,pF$; ${}^{h}C_m + 0.5\,pF$; ${}^{h}C_m - 0.5\,pF$; ${}^{L}C_m \times 0.96$, and ${}^{h}C_m \times 0.96$. In all cases the errors in the resulting estimated offset curves were small at the biomass measuring frequency of 0.4 MHz.

Values for ${}^{L}f$, ${}^{h}f$ and the biomass measuring frequency of 0.20, 0.28 and 0.40 MHz, respectively, seem to work extremely well. If a BM was set-up to do simple biomass measurements it would take spot cell suspension readings at these three frequencies only and estimate ${}^{L}C_p$ using Eq. (3). It would then estimate the polarisation at 0.4 MHz (${}^{0.4\,MHz}C_p$) using Eq. (4) which because of the fixed known frequencies used becomes ${}^{0.4\,MHz}C_p = {}^{L}C_p \times 0.23981$. This ${}^{0.4\,MHz}C_p$ would then be subtracted from the capacitance actually measured at 0.4 MHz for the cell suspension to give the value corrected for polarisation. This can easily be implemented on a PC.

The simulations produced good evidence that the 2f method would perform well with realistic offset changes, even with noise present. However, for it to be implemented in a practical situation (e.g., inside a BM) one would like to model how any errors due to offset changes propagate through the method so that predictions of the effects could be made in a thorough and systematic manner.

### *3.3. Modelling the effect of a sloping offset under the polarisation on the 2f method*

#### *3.3.1. Defining the approach to the error model*

The aim of the error model was to quantify the percentage error in the *polarisation curve* estimated using the 2f model when the offset changes between the ${}^{L}f$ and ${}^{h}f$. Fig. 2 illustrates the effect of such an offset change on the polarisation estimated by the model. The correct polarisation curve is shown as line (d) which has the correct ${}^{L}f$ magnitude, ${}^{L}C_p$. Because of the change in the offset, what the 2f model actually gives is line (e). The aim is to express the difference between the polarisation lines (e) and (d) as a percentage of the correct values given by line (d). One thus gets a percentage error in the estimated *polarisation* as a function of frequency (${}^{f}E_p$) which is given by:

$$ {}^{f}E_p = \frac{{}^{f}C_p \text{ with offset error} - {}^{f}C_p \text{ without offset error}}{{}^{f}C_p \text{ without offset error}} \times \frac{100}{1} \qquad (5) $$

Where 'offset error' is the error resulting from a non-constant offset. Each of the ${}^{f}C_p$ terms in this equation has the form of Eq. (4) with the same values of ${}^{L}f$ and ${}^{h}f$ because these values are assumed to be known constants when using the 2f method. This in turn means that the power of 2 terms in Eq. (4) are the same with and without the offset error. What differs between the polarisation curves with and without offset error is the magnitude of the ${}^{L}C_p$ the 2f model gives. Fig. 5a shows lines (d) and (e) from Fig. 2 in more detail, with the notation used in these derivations. The thick line is the correct polarisation curve and has the correct ${}^{L}C_p$ and ${}^{f}C_p$ values. The thin line curve represents the polarisation curve the 2f model gives when the offset is not constant between ${}^{L}f$ and ${}^{h}f$ (i.e., with offset error present). The additional 'a,Δo' terms in the

subscripts indicate that the values are (calculated) apparent values due to the change in the offset capacitance. From these arguments one can see that the '${}^{f}C_{p}$ without offset error' terms in Eq. (5) can be replaced by Eq. (4). The '${}^{f}C_{p}$ with offset error' terms are replaced by the modified form of Eq. (4):

$$ {}^{f}C_{p,a\Delta o} = {}^{L}C_{p,a\Delta o}\, 2^{(\log({}^{L}f/f)/\log({}^{h}f/{}^{L}f))} \quad (6) $$

To calculate the ${}^{f}C_{p,a\Delta o}$ to insert into Eq. (5) one needs to find an equation for ${}^{L}C_{p,a\Delta o}$ which includes the change in the offset capacitance between ${}^{L}f$ and ${}^{h}f$.

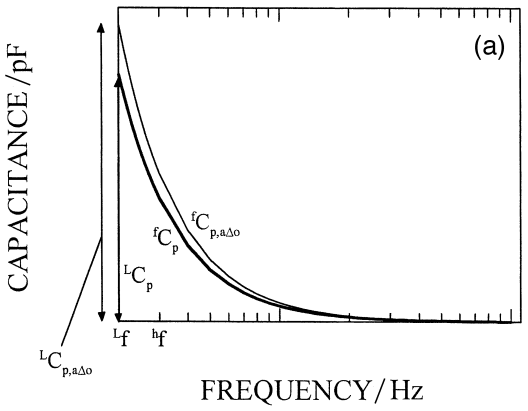


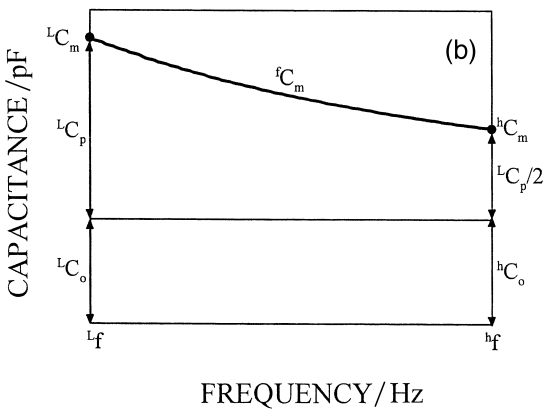


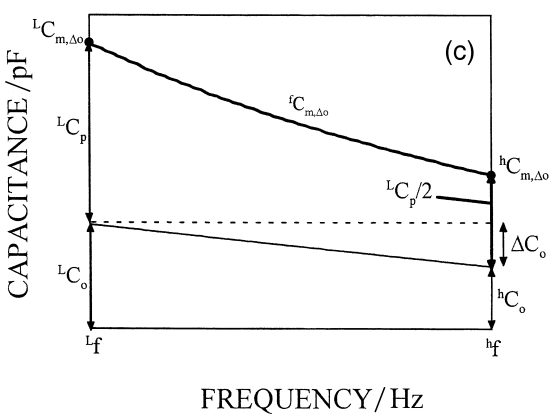


Fig. 5. (a) The polarisation curves given by the 2f method. The thick line shows how the true polarisation changes with frequency (${}^{f}C_{p}$) and has a true ${}^{L}f$ capacitance of ${}^{L}C_{p}$. The fact that the offset is not constant between ${}^{L}f$ and ${}^{h}f$ has resulted in the 2f method overestimating the magnitude of the capacitance at ${}^{L}f$ (${}^{L}C_{p,a}\Delta_{o}$) and this has resulted in the frequency dependence (${}^{f}C_{p,a}\Delta_{o}$) shown by the thin line. (b) The segment of a measured suspension's capacitance curve (${}^{f}C_{m}$) when the offset is the same at ${}^{L}f$ and ${}^{h}f$ (${}^{L}C_{o}$ and ${}^{h}C_{o}$, respectively). Under such perfect conditions inserting the measured capacitances at ${}^{L}f$ and ${}^{h}f$ (${}^{L}C_{m}$ and ${}^{h}C_{m}$, respectively) into the 2f model will give the correct value for ${}^{L}C_{p}$ and its frequency dependence (thick line on a). (c) The plot in (b) but this time the offsets at ${}^{L}f$ and ${}^{h}f$ differ causing the measured capacitances (${}^{f}C_{m,}\Delta_{o}$) to fall more steeply even though the actual polarisation has the same ${}^{L}C_{p}$ and frequency dependence as before. The change in the offset between ${}^{L}f$ and ${}^{h}f$ is called $\Delta C_{o}$. Inserting the measured capacitances at ${}^{L}f$ and ${}^{h}f$ (${}^{L}C_{m,}\Delta_{o}$ and ${}^{h}C_{m,}\Delta_{o}$, respectively) into the 2f model results in the over estimated apparent value of ${}^{L}C_{p}$ (${}^{L}C_{p,a}\Delta_{o}$) and its frequency dependence seen as the thin line on (a).

*3.3.2. Finding an equation for ${}^{L}C_{p,a\Delta o}$*

Fig. 5b shows the segment of a cell suspension's capacitance plot between ${}^{L}f$ and ${}^{h}f$ with the offset capacitances being equal at the two frequencies. From this situation one may vary the offset capacitances in four ways: keep ${}^{L}C_{o}$ constant and increase or decrease ${}^{h}C_{o}$, or keep ${}^{h}C_{o}$ constant and increase and decrease ${}^{L}C_{o}$.

Taking first the case where ${}^{L}C_{o}$ is held constant. Fig. 5c shows what happens to Fig. 5b when the ${}^{h}C_{o}$ is lowered. The true ${}^{L}C_{p}$ and ${}^{L}C_{p}/2$ values are the same, what changes are the measured capacitance values. These values are flagged to show that they pertain to the situation of a changing offset (between ${}^{L}f$ and ${}^{h}f$) by having 'Δo' appended to their subscripts. Thus the capacitances a BM would measure under these conditions is called ${}^{f}C_{m,\Delta o}$ and the spot capacitances at ${}^{L}f$ and ${}^{h}f$ are called ${}^{L}C_{m,\Delta o}$ and ${}^{h}C_{m,\Delta o}$, respectively. One defines the change in the offset capacitance between ${}^{L}f$ and ${}^{h}f$ as the $\Delta C_{o}$ shown on Fig. 5c. This is given by Eq. (7):

$$ \Delta C_{o} = {}^{h}C_{o} - {}^{L}C_{o} \quad (7) $$

From Fig. 5c we see that the measured capacitance at ${}^{L}f$ is given by:

$$ {}^{L}C_{m,\Delta o} = {}^{L}C_{o} + {}^{L}C_{p} \quad (8) $$

The measured capacitance at ${}^{h}f$ is given by:

$$ {}^{h}C_{m,\Delta o} = {}^{L}C_{o} + \Delta C_{o} + \frac{{}^{L}C_{p}}{2} \quad (9) $$

In fact both Eqs. (8) and (9) also apply to the situation where ${}^{L}C_{o}$ is constant but ${}^{h}C_{o}$ is increased. Next one subtracts Eq. (9) from Eq. (8) to give:

$$ {}^{L}C_{m,\Delta o} - {}^{h}C_{m,\Delta o} = \frac{{}^{L}C_{p}}{2} - \Delta C_{o} \quad (10) $$

Next we repeat the above procedure for the case where the ${}^{h}C_{o}$ is constant but the ${}^{L}C_{o}$ is either increased or decreased. Once again the derived equations for the mea-

sured capacitances at these two spot frequencies apply in both cases and are:

$$^{L}C_{m,\Delta o} = {}^{h}C_o + (-\Delta C_o) + {}^{L}C_p \quad (11)$$

$$^{L}C_{m,\Delta o} = {}^{h}C_o + \frac{^{L}C_p}{2} \quad (12)$$

Subtracting Eq. (12) from Eq. (11) once again gives Eq. (10). Thus one can use Eq. (10) for all the possible situations where the offset changes between $^{L}f$ and $^{h}f$.

In reality when we make a 2f method measurement we measure $^{L}C_m$ and $^{h}C_m$ at $^{L}f$ and $^{h}f$ and insert these values into Eq. (3); which assumed no offset changes (error), to get the correct value of $^{L}C_p$. Now if an offset error was present we would again just take spot capacitance readings at $^{L}f$ and $^{h}f$ to give this time $^{L}C_{m,\Delta o}$ and $^{h}C_{m,\Delta o}$. Inserting these values into Eq. (3) instead of $^{L}C_m$ and $^{h}C_m$ gives:

$$^{L}C_{p,a\Delta o} = 2\left(^{L}C_{m,\Delta o} - {}^{h}C_{m,\Delta o}\right) \quad (13)$$

The estimated $^{L}C_p$ is now called $^{L}C_{p,a\Delta o}$ (see Fig. 5a) to remind us that the calculated $^{L}C_p$ is an apparent one due to errors caused by changes in the offset capacitances which we have not allowed for by blindly using the 2f model. One can replace the bracketed terms in Eq. (13) by substituting in Eq. (10) to give:

$$^{L}C_{p,a\Delta o} = 2\left(\frac{^{L}C_p}{2} - \Delta C_o\right) \quad (14)$$

We now have an explicit statement of $^{L}C_{p,a\Delta o}$ to insert into Eq. (6) to give:

$$^{f}C_{p,a\Delta o} = 2\left(\frac{^{L}C_p}{2} - \Delta C_o\right)2^{(\log(^{L}f/f)/\log(^{h}f/^{L}f))} \quad (15)$$

### 3.3.3. Calculating $^{f}E_p$

Eq. (5) gives an explicit statement of $^{f}E_p$. Its '$^{f}C_p$ without offset error' terms can be replaced by Eq. (4) while the '$^{f}C_p$ with offset error' terms are replaced by Eq. (15). Making these substitutions into Eq. (5) and then simplifying gives Eq. (16):

$$^{f}E_p = -2\left(\frac{\Delta C_o}{^{L}C_p}\right)\frac{100}{1} \quad (16)$$

where $^{L}C_p$ is the correct $^{L}C_p$ value (e.g., line d on Fig. 2).

Note that the percentage error in the estimated polarisation ($^{f}E_p$) is frequency-independent, thus the difference between lines (e) and (d) on Fig. 2 is always the same proportion of (d). The size of this percentage error is given by the ratio of the change in the offset between $^{L}f$ and $^{h}f$ (namely $\Delta C_o$), to the correct magnitude of the polarisation at $^{L}f$ (namely $^{L}C_p$). Thus if $\Delta C_o$ is a hundredth of $^{L}C_p$ the two-frequency method produces a frequency independent 2% error in the calculated $^{f}C_p$ values. In addition offsets that slope down have negative $\Delta C_o$s and so cause an overestimation of the polarisation.

It is important to remember that polarisation curves such as line (e) on Fig. 2, which contain an error due to a non-constant offset, do not cause significant problems for biomass estimation. When line (e) is subtracted from the measured suspension data one gets line (c) rather than the correct line (b), but by the biomass measuring frequency the difference between the two lines is usually quite small (and hopefully small compared to the value of line (b) at that frequency).

### 3.4. Experimental application of the 2f method to yeast suspensions

Suspensions of live yeast were made up and scanned on a BM in high and low cell constant modes using the mAu probe, as described in Section 2. To access the shape of the polarisation curves, the polarisation control data were fitted to the power law and the $^{h}f$ and $^{L}C_p$ (relative to an $^{L}f$ of 0.2 MHz) calculated as in Ref. [1]. The power law fits were very good in both high and low cell constant modes and yielded $^{h}f$ values of 0.29 and 0.28 MHz receptively. Thus even though this experiment was done some five months after the previously described one, the $^{h}f$ had not changed. In addition the $^{h}f$ values were the same irrespective of which cell constant modes were used.

Fig. 6a and b show the frequency scan data for the high and low cell constants, respectively. On each plot are shown the raw suspension scans along with their equivalent polarisation controls. Conventional polarisation controls were applied to the data by subtracting the polarisation control data from the suspension data. The polarisation control data's capacitance at 1 MHz was added back to the resulting curves to allow them to be plotted in comparison with the original data. From Fig. 6a and b one can see that this has largely eliminated the polarisation tip-up at low frequencies. The problem with polarisation controls is that they also compensate for the sloping BM baseline and the high-frequency inductance effects. This explains why the data compensated using them have a different shape at higher frequencies. The 2f method does not compensate for baseline slopes or the high-frequency inductances and so a better way of comparing data would be to extract just the polarisation component from the polarisation control data and subtract this from the cell suspension data. This can be done by using the power law fits to the polarisation in the polarisation control data (as was done in Figs. 3 and 4 in Ref. [1]) to generate data values at each frequency used, as was done on Fig. 5 in Ref. [1]. These data can then be subtracted from the raw cell suspension data. The resulting plots are also shown on Fig. 6a and b. As would be expected they follow the conventional polarisation controlled data at low frequencies and follow the cell suspension data at the higher frequencies where the polarisation is no longer seen.

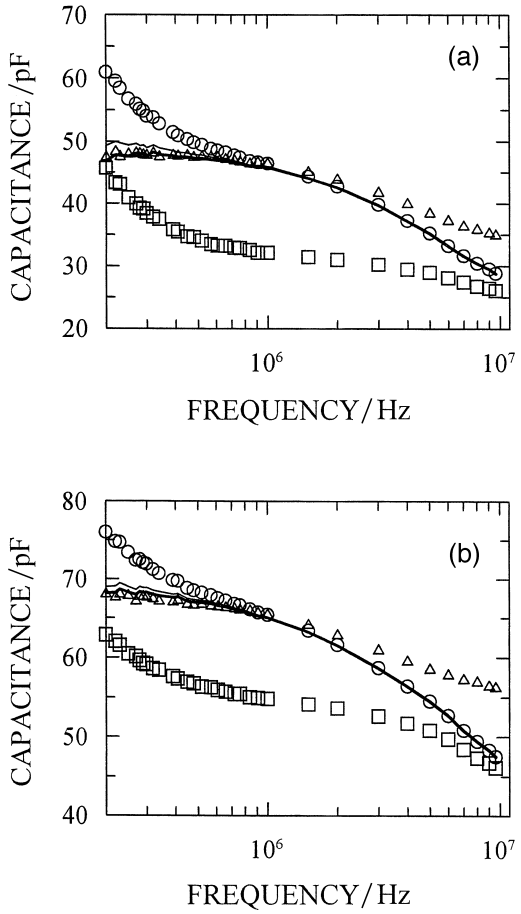


Fig. 6. The application of the 2f method to real suspensions of yeast with the BM in high (a) and low (b) cell constant modes. On both plots the circles are the ('raw') yeast suspension data as measured and the squares are the equivalent polarisation control data. The triangles are the result of subtracting the polarisation control data from the yeast suspension data and then adding the polarisation control capacitance at 1 MHz back to all the frequencies used. The thick line is the result of fitting a power law to the polarisation in the polarisation control data and then subtracting this fit from the yeast suspension data. The thin line is the result of applying the 2f method to reduce the polarisation.

The final set of data was obtained by applying the 2f method of removing electrode polarisation to the raw cell suspension data using a ${}^{L}f$ and ${}^{h}f$ of 0.20 and 0.28 MHz, respectively, exactly as described before. For both Fig. 6a and b the differences between the three sets of polarisation compensated data at low frequencies is extremely small. None of the compensation methods can be regarded as the 'gold standard' as they all involve approximations. For those methods using measured polarisation control data the subtraction process is applying to a serial combination of electrode impedance and suspension impedance a method strictly applicable only to a parallel arrangement of these two impedances [10]. The method only works well because of the fortuitous values these impedances take for typical electrode/suspension systems and in our experience tends to over- or underestimate the polarisation at high conductances. Thus some error is to be expected. The fact that the baseline of the BM slopes down and that the β-dispersion of the yeast will also produce a sloping offset suggests, from the analysis of sloping offsets earlier, that the real polarisation-free curve may plateau slightly above the 2f method's curves shown. In any case all the polarisation compensated data do appear by eye to fit well with the breakpoint in the suspension data at about 1 MHz, below which the polarisation causes the curve to tip-up.

### *3.5. Modifications to the 2f method*

For most situations the 2f method of electrode polarisation reduction will work well and has the virtue of simplicity. There may be times however when a sloping offset could produce severe problems for biomass measurements, and frequency scans in particular. Under these conditions the 2f method could be enlarged to a three frequency method which would model the offset as a sloping straight line with the offset capacitances at the three frequencies sitting on it. Similar simultaneous equations (equivalent to Eqs. (1)–(4)) as used in the 2f method could then be solved to allow for this slope. The three frequencies would need to be close together to ensure that the offset capacitances do lie roughly on a straight line and such a method may be easier to derive using $p$ [1] directly rather than using constant ${}^{L}f$ and ${}^{h}f$ values and, say, an equivalent three quarters frequency.

For situations where the ${}^{h}f$ and ${}^{L}C_{p}$ are both variable one could use a 3-frequency method that assumed that the offset capacitance was constant at the three frequencies. One could then solve the simultaneous equations for ${}^{h}f$ and ${}^{L}C_{p}$. We have already derived the equations required to implement both the three-frequency methods alluded to above. Four or more frequencies could be used if one wished to model the changing offset under the polarisation curve by a more complex and realistic function.

It is possible that for some systems the power term $p$ may have a given constant value only within a given (broad) frequency range and that different values will be required for different frequency ranges (see the data in Ref. [10] and the polarisation impedance data in Ref. [8]). Under these conditions the 2f method can be applied separately to a series of overlapping frequency windows.

## 4. Concluding remarks

A useful consequence of the constant ${}^{h}f$ for the BM demonstrated in the previous paper [1] is that spot measurements at two frequencies can be used to compensate for electrode polarisation using the 2f method developed in this paper. This method was shown by simulation and with real suspensions to provide reliable biomass measurements even when its key assumption of a constant offset was violated. For general applications one would use a spot biomass measuring frequency which was higher than the

two frequencies used by the 2f method, to reduce any errors caused by the non-constant offset. For most practical situations the 2f method would seem to provide as good a removal of electrode polarisation on frequency scans as conventional polarisation control methods give. For cases where a sloping offset causes severe problems or where the ${}^{h}f$ moves then modifications of the 2f idea using 3 or more frequencies may be used.

To use the 2f method the polarisation must follow a power (or similar) law and have a constant known ${}^{h}f$ value. If these requirements are met the technique can be applied to any electrode system not just those of the BM and the equations were derived so that they were not absolutely specific to the BM. Indeed the method can be applied to any situation where electrode polarisation is a problem including dispersions other than the β-dispersion and to materials other than biological ones.

Applied to the current range of BMs the 2f method is easy to implement on a controlling computer and the stability of the ${}^{h}f$ value means that experiment-by-experiment recalibration would not be required. Once implemented the results would be on-line, real-time, relatively resistant to noise and would require no expert intervention from the users.

## Acknowledgements

We thank the BBSRC and the Wellcome Trust for financial support and Drs. Hazel Davey, Andrew Woodward, Mark Spittle and Robert Todd for useful discussions.

## Appendix A

### Calculating the frequency dependence of the polarisation

Eq. A1.3 in Ref. [1] is rearranged for $p$ and then substituted into Eq. A1.2 in Ref. [1]; which is the alternative form of the linearised power law, to give:

$$\log\left({}^{f}C_{\mathrm{p}}\right) = \log\left({}^{\mathrm{L}}C_{\mathrm{p}}\right) - \frac{\log(2)}{\log\left({}^{\mathrm{h}}f/{}^{\mathrm{L}}f\right)}\log\left(f/{}^{\mathrm{L}}f\right) \qquad \text{(A1.1)}$$

Anti-logging both sides and simplifying gives Eq. (4).

## References

[1] C.L. Davey, D.B. Kell, The influence of electrode polarisation on dielectric spectra, with special reference to capacitive biomass measurements: I. Quantifying the effects on electrode polarisation of factors likely to occur during fermentations, Bioelectrochem. Bioenerg. 46 (1998) 91–103.

[2] I. Cerckel, A. Garcia, V. Degouys, D. Dubois, L. Fabry, A.O.A. Miller, Dielectric-spectroscopy of mammalian-cells: 1. Evaluation of the biomass of Hela-Cell and CHO-Cells in suspension by low-frequency dielectric-spectroscopy, Cytotechnology 13 (1993) 185–193.

[3] V. Degouys, I. Cerckel, A. Garcia, J. Harfield, D. Dubois, L. Fabry, A.O.A. Miller, Dielectric spectroscopy of mammalian cells: 2. Simultaneous in situ evaluation by aperture impedance pulse spectroscopy and low-frequency dielectric spectroscopy of the biomass of HTC cells on Cytodex 3, Cytotechnology 13 (1993) 195–202.

[4] S.A. Siano, Biomass measurement by inductive permittivity, Biotechnol. Bioeng. 55 (1997) 289–304.

[5] D.B. Kell, The principles and potential of electrical admittance spectroscopy: an introduction, in Biosensors: Fundamentals and Applications, Oxford University Press, Oxford, 1987, pp. 427–468.

[6] E.H. Grant, R.J. Sheppard, G.P. South, Dielectric Behaviour of Biological Molecules in Solution, Clarendon Press, Oxford, 1978.

[7] H.P. Schwan, Determination of biological impedances., in Physical Techniques in Biological Research, Academic Press, New York, Vol. VIB, 1963, pp. 323–407.

[8] B. Onaral, H.H. Sun, H.P. Schwan, Electrical properties of bioelectrodes, IEEE Trans. Biomed. Eng. BMI 31 (1984) 827–832.

[9] R. Pethig, D.B. Kell, The passive electrical properties of biological systems: their significance in physiology, biophysics and biotechnology, Phys. Med. Biol. 32 (1987) 933–970.

[10] C.L. Davey, G.H. Markx, D.B. Kell, Substitution and spreadsheet methods for analysing dielectric spectra of biological systems, Eur. Biophys. J. 18 (1990) 255–265.

[11] C.L. Davey, D.B. Kell, R.B. Kemp, R.W.J. Meredith, On the audio- and radio-frequency dielectric behaviour of anchorage-independent, mouse L929-derived LS fibroblasts, Bioelectrochem. Bioenerg. 20 (1988) 83–98.

[12] A.M. Woodward, A. Jones, Z. Xin-zhu, J. Rowland, D.B. Kell, Rapid and non-invasive quantification of metabolic substrates in biological cell suspensions using non-linear dielectric spectroscopy with multivariate calibration and artificial neural networks. Principles and applications, Bioelectrochem. Bioenerg. 40 (1996) 99–132.

[13] M. Watanabe, T. Suzaki, A. Irimajiri, Dielectric behavior of the frog lens in the 100 Hz to 500 MHz range: simulation with an allocated ellipsoidal shells model, Biophys. J. 59 (1991) 139–149.

[14] H.P. Maruska, J.G. Stevens, Technique for extracting dielectric permittivity from data obscured by electrode polarisation, IEEE Trans. Electrical Insul. 23 (1988) 197–200.

[15] C.M. Harris, R.W. Todd, S.J. Bungard, R.W. Lovitt, J.G. Morris, D.B. Kell, The dielectric permittivity of microbial suspensions at radio-frequencies: a novel method for the estimation of microbial biomass, Enzyme Microbial Technol. 9 (1987) 181–186.

[16] H.P. Schwan, C.D. Ferris, Four-terminal null techniques for impedance measurement with high resolution, Rev. Sci. Instrum. 39 (1968) 481–485.

[17] C.D. Ferris, Introduction to Bioelectrodes, Plenum Press, New York, 1974.

[18] D.B. Kell, C.L. Davey, Conductimetric and impedimetric devices, in Biosensors: a Practical Approach, IRL Press, Oxford, 1990, pp. 125–154.

[19] C.L. Davey, Y. Guan, R.B. Kemp, D.B. Kell, Real-time monitoring of the biomass content of animal cell cultures using dielectric spectroscopy, in: K. Funatsu et. al (Eds.), Animal Cell Technology Basic and Applied Aspects, Proceedings of the Japanese Association of Animal Cell Technology, Vol. 8, 1997, pp. 61–65.

[20] D.B. Kell, C.L. Davey, On fitting dielectric spectra using artificial neural networks, Bioelectrochem. Bioenerg. 28 (1992) 425–434.

[21] D.J. Nicholson, D.B. Kell, C.L. Davey, Deconvolution of the dielectric spectra of microbial cell suspensions using multivariate calibration and artificial neural networks, Bioelectrochem. Bioenerg. 39 (1996) 185–193.

[22] C.L. Davey, D.B. Kell, The low-frequency dielectric properties of biological cells, Bioelectrochemistry of cells and tissues, Birkauser, Zurich, 1995, pp. 159–207.